Supporting Information

Formation of Square Lamellae

by Self-Assembly of Long-Chain Bolaphospholipids in Water

Annette Meister,*[a] Simon Drescher,[b] Göran Karlsson,[c] Gerd Hause,[d] Ute Baumeister,[a] Günter Hempel,[e] Vasil M. Garamus,[f] Bodo Dobner,[b] Alfred Blume[a]

[a] *Institute of Chemistry, Physical Chemistry, MLU Halle-Wittenberg, Von-Danckelmann-Platz 4, 06120 Halle, Germany,*

[b] *Institute of Pharmacy, Biochemical Pharmacy, MLU Halle-Wittenberg, Wolfgang-Langenbeck-Str. 4, 06120 Halle, Germany,*

[c] *Department of Physical and Analytical Chemistry, Uppsala University, 75123 Uppsala, Sweden,*

[d] *Biocenter, MLU Halle-Wittenberg, Weinbergweg 23, 06120 Halle, Germany,*

[e] *Institute of Physics, MLU Halle-Wittenberg, Betty-Heimann-Str. 7, 06120 Halle, Germany,*

[f] *GKSS Research Centre, Max-Planck-Str., 21502 Geesthacht, Germany*

* To whom correspondence should be addressed: annette.meister@chemie.uni-halle.de

Experimental Section

Materials

The purity of all compounds and products was checked by thin layer chromatography (TLC plates; *Merck*, Darmstadt, Germany). The purification of the bolaamphiphiles was carried out by middle pressure liquid chromatography (MPLC; Cartriger C-670, Fraction Collector C-660, Pump Module C-601, Pump Manager C-615, *Büchi*, Essen, Germany) using silica gel 60 (0.040–0.063 mm, *Merck*, Darmstadt, Germany) and chloroform/methanol/water as eluent (gradient technique). Melting points are uncorrected and were determined with a Boetius apparatus. NMR spectra were obtained using a Varian Inova 500 or Varian Gemini 2000 NMR spectrometer with $CDCl_3$ and CD_3OD as internal standards. Mass spectrometric data were obtained with a Finnigan mass spectrometer model MAT SSQ 710 C (ESI-MS; *Thermo Separation Products*, San José, CA, USA and *Thermoquest*, Engelsbach, Germany) or were recorded on an AMD 402 spectrometer (EI-MS; 70 eV, *AMD Intecta GmbH*, Harpstedt, Germany). Elemental analyses were performed with a Leco CHNS- 932 (*Leco-Corporation*, St. Joseph, MI, USA). All solvents were purified and dried before use. Commercially available reagents were supplied by *Aldrich Co* (Steinheim, Germany) and were used without further purification. The perdeuterated 1,12-dibromododecane (**2c**) was supplied by *CDN-Isotopes* (*Dr. Ehrenstorfer GmbH*, Augsburg, Germany). Sodium acetate and acetic acid (100%) were purchased from *Merck* (Darmstadt, Germany) and *Riedel-de Haën* (Seelze, Germany), respectively. ^{2}H- and ^{31}P-NMR measurements were performed in deuterium depleted water. For the SANS measurements D_2O from Isotec Inc. (Miamisburg, OH, USA) was used. The bolalipids PC-Cn-PC (n = 34, 36), Me_2PE-Cn-Me_2PE (n = 34, 36), dPC-C34-PC and dMe_2PE-C34-Me_2PE were synthesized according to the procedure described below. Deuterated bolalipids were synthesized to get additional information about the conformation and mobility of the alkyl chain within the aggregates by FT-IR, SANS and ^{2}H-NMR measurements.

Sample preparation

The appropriate amount of the bolalipid was suspended in water or 10 mM acetate buffer at pH 5 for DSC, TEM and SANS measurements (H_2O: DSC, TEM; D_2O: SANS) or in 300 mM acetate buffer for FT-IR, ^{2}H- and ^{31}P-NMR measurements (H_2O: NMR, FT-IR). Homogenous dispersions were obtained by heating to 90 °C and vortexing of the sample.

Synthesis
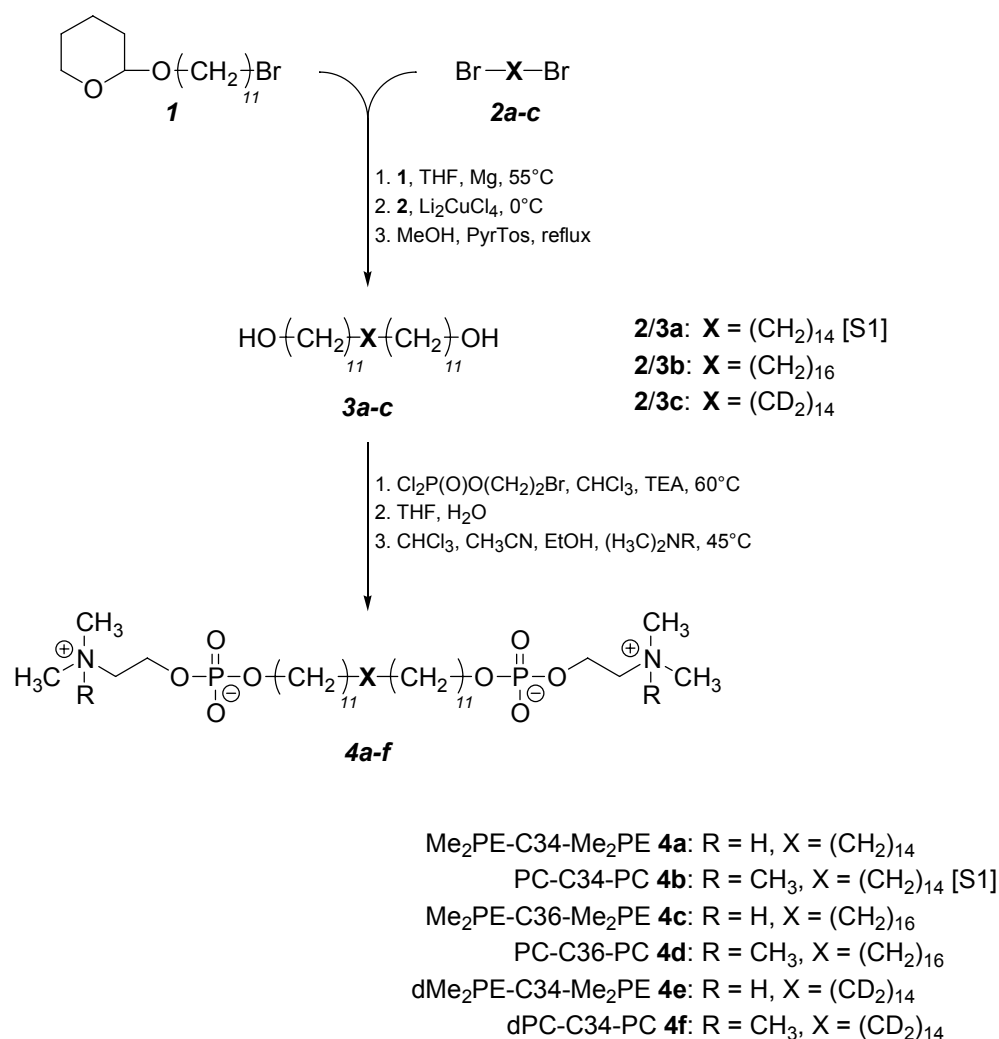
Scheme 1 Synthetic pathway for the preparation of long-chain bolaamphiphiles.

Copper-catalyzed GRIGNARD coupling

The 1,ω-diols **3a-c** were synthesized by copper-catalyzed GRIGNARD coupling [S2, S3]. A solution of 11-bromo-1-[(tetrahydro-2*H*-pyran-2-yl)oxy]undecane **1** in dry THF (50 ml) was added dropwise to magnesium turnings under argon atmosphere. After the exothermic reaction had subsided, the mixture was stirred at 55 °C for 3 h. The excess magnesium was removed by filtration and the GRIGNARD solution was cooled to – 5 °C. A freshly prepared solution of dilithium tetrachlorocuprate(II) (0.1M in THF, 3.5 ml) was added with stirring. After a solution of 1,ω-dibromoalkane **2** in dry THF (50 ml) was added in one portion, stirring was continued for further 3 h at 0 °C. For the work-up diethyl ether (150 ml) was added and the resulting mixture was poured into a cold saturated solution of ammonium chloride

(150 ml). The organic layer was separated and the aqueous phase was extracted with diethyl ether (2× 50 ml). The combined organic phases were washed with water, dried over sodium sulfate and concentrated to dryness under reduced pressure. For cleavage of the THP protecting groups the crude bis(tetrahydropyranyl ether) were dissolved in dry methanol (100 ml) and heated under reflux for 3 h with catalytic amounts of pyridinium p-toluene sulfonate. The hot suspension was filtered and the residue was recrystallised from heptane to give the pure 1,ω-diols **3** as white crystals.

The analytical data of tetratriacontane-1,34-diol **3a** are described in [S1].

Hexatriacontane-1,36-diol **3b** was obtained from **1** (20.1 g, 60 mmol) and 1,14-dibromotetradecane **2b** (7.12 g, 20 mmol). Yield: 7.22 g (67%); m.p. 116.0 °C; ^{1}H-NMR (400 MHz, CDCl$_3$, 27 °C): δ = 1.21–1.31 (m, 64H; HO(CH$_2$)$_2$(CH_2)$_{32}$(CH$_2$)$_2$OH), 1.51–1.55 (m, 4H; HOCH$_2$CH_2(CH$_2$)$_{32}$CH_2CH$_2$OH), 3.62 ppm (t, ^3J(H,H)=6.6 Hz, 4H; 2× HOCH_2−); MS (EI, 70 eV): m/z (%): 538 (4) [M^+], 502 (36) [M^+–2H$_2$O]; elemental analysis calcd (%) for C$_{36}$H$_{74}$O$_2$ (538.97): C 80.22, H 13.84; found: C 80.04, H 14.09.

Tetratriacontane-(12,12,13,13,14,14,15,15,16,16,17,17,18,18,19,19,20,20,21,21,22,22,23,23-[D$_{24}$])-1,34-diol **3c** was obtained from **1** (3.8 g, 11.3 mmol) and perdeuterated 1,12-dibromo-dodecane **2c** (1.0 g, 2.8 mmol). Yield: 0.67 g (44%); m.p. 111.6–112.3 °C; ^{1}H-NMR (400 MHz, CDCl$_3$, 27 °C): δ = 1.22–1.56 (m, 40H; 2× HOCH$_2$(CH_2)$_{10}$−), 3.59 ppm (t, ^3J(H,H)=6.6 Hz, 4H; 2× HOCH_2−); MS (EI, 70 eV): m/z (%): 535 (3) [M^+], 498 (43) [M^+–2H$_2$O].

General procedures for phosphorylation and quarternisation reaction

β-Bromoethylphosphoric acid dichloride (0.97 g, 4 mmol) was poured into dry chloroform (15 ml) under cooling with an ice-water solution. A mixture of dry TEA (0.71 g, 7 mmol) with dry chloroform (15 ml) was added slowly under stirring which was continued for 30 min at 0 °C. The 1,ω-diol **3** (0.5 mmol) was added as solid substance in one portion. The suspension was heated up to 60 °C until the solid was dissolved. Stirring was continued for further 24–48 h at room temperature. After TLC (CHCl$_3$/Et$_2$O = 8/2, v/v) showed complete conversion of the 1,ω-diol **3,** crushed ice (30 ml) was added to the solution and the mixture was stirred for further 2 h. The organic layer was separated and the aqueous phase was diluted with a cold saturated solution of sodium chloride (30 ml) and then extracted with chloroform

($2\times$ 50 ml). The combined organic phases were concentrated under reduced pressure and the oily residue was dissolved in THF/H_2O (9/1, v/v, 15 ml). After 1.5 h the solvent was evaporated and the oily residue was transferred into a mixture of chloroform (15 ml), acetonitrile (15 ml) and an ethanolic solution of trimethylamine (5 ml, 4.2M), or dimethylamine (5 ml, 5.6M), respectively. The mixture was kept in a closed tube at 40–45 °C for 48–72 h. After TLC ($CHCl_3$/MeOH/ammonia = 50/50/10 or 50/50/15, v/v/v) showed the formation of the product, the mixture was concentrated by evaporation of the solvent and the residue purified by middle pressure liquid chromatography (MPLC) on silica gel using the gradient technique and chloroform/methanol/water as eluent. The bolaamphiphiles **4** were dried in vacuo over phosphorus pentoxide at room temperature for 2 days. For physico-chemical studies the products were dissolved in a small amount of dry chloroform/methanol (1/1, v/v). Dry acetone was then added to precipitate the white product. The precipitate was separated from eluent by centrifugation and dried in vacuo over phosphorus pentoxide.

Tetratriacontane-1,34-diyl-bis[2-(dimethylammonio)ethylphosphate] (**4a**). Yield: 0.28 g (69%); ^{1}H-NMR (400 MHz, $CDCl_3$/CD_3OD, 27 °C): δ = 1.20–1.30 (m, 60H, $-O(CH_2)_2$ $(CH_2)_{30}(CH_2)_2O-$), 1.53–1.60 (m, 4H, $-OCH_2CH_2(CH_2)_{30}CH_2CH_2O-$), 2.81 (s, 12H, $4\times$ $-CH_3$), 3.16–3.18 (m, 4H, $2\times$ NCH_2CH_2O-), 3.82 (q, J=6.6 Hz, 4H, $-OCH_2(CH_2)_{32}CH_2O-$), 4.10–4.14 ppm (m, 4H, $2\times$ NCH_2CH_2O-); ^{13}C-NMR (100 MHz; $CDCl_3$/CD_3OD, 27°C): δ = 25.65 ($2\times$ $-O(CH_2)_2CH_2(CH_2)_{14}-$), 29.24 ($2\times$ $-O(CH_2)_{16}CH_2-$), 29.51–29.56 ($2\times$ $-O(CH_2)_3$ $(CH_2)_{13}CH_2-$), 30.59 (d, ^3J(C,P)=7.7 Hz, $2\times$ $-OCH_2CH_2(CH_2)_{15}-$), 43.26 ($4\times$ $-CH_3$), 58.81–59.02 ($2\times$ NCH_2CH_2O-), 66.12 ppm (d, ^2J(C,P)=6.1 Hz, $2\times$ $-OCH_2(CH_2)_{16}-$); MS (ESI): m/z: 811.8 [M^+–H], 813.7 [M^++H], 835.6 [M^++Na]; elemental analysis calcd. (%) for $C_{42}H_{90}N_2O_8P_2 \cdot 1\ H_2O$: C 60.69, H 11.16, N 3.37; found: C 60.59, H 10.84, N 3.42.

The analytical data of tetratriacontane-1,34-diyl-bis[2-(trimethylammonio)ethylphosphate] (**4b**) are described in [S1].

Hexatriacontane-1,36-diyl-bis[2-(dimethylammonio)ethylphosphate] (**4c**). Yield: 0.57 g (68%); ^{1}H-NMR (400 MHz, $CDCl_3$/CD_3OD, 27 °C): δ = 1.19–1.29 (m, 64H, $-O(CH_2)_2$ $(CH_2)_{32}(CH_2)_2O-$), 1.52–1.59 (m, 4H, $-OCH_2CH_2(CH_2)_{32}CH_2CH_2O-$), 2.80 (s, 12H, $4\times$ $-CH_3$), 3.15–3.17 (m, 4H, $2\times$ NCH_2CH_2O-), 3.80 (q, J=6.6 Hz, 4H, $-OCH_2(CH_2)_{34}CH_2O-$), 4.08–4.13 (m, 4H, $2\times$ NCH_2CH_2O-); ^{13}C-NMR (100 MHz, $CDCl_3$/CD_3OD, 27°C): δ = 25.71 ($2\times$ $-O(CH_2)_2CH_2(CH_2)_{15}-$), 29.29 ($2\times$ $-O(CH_2)_{17}CH_2-$), 29.52–29.59 ($2\times$ $-O(CH_2)_3(CH_2)_{14}$ CH_2-), 30.67 (d, ^3J(C,P)=7.4 Hz, $2\times$ $-OCH_2CH_2(CH_2)_{16}-$), 43.56 ($4\times$ $-CH_3$), 58.67, 58.69,

58.73, 58.74, 59.36 and 59.41 (2× NCH_2CH_2O−), 66.13 (d, ^2J(C,P)=5.9 Hz, 2× −OCH_2(CH$_2$)$_{17}$−); MS (ESI): *m/z*: 839.8 [M$^+$−H], 1680.7 [2M$^+$−2H], 842.3 [M$^+$+H], 863.8 [M$^+$+Na]; elemental analysis calcd. (%) for C$_{44}$H$_{94}$N$_2$O$_8$P$_2$·1 H$_2$O: C 61.51, H 11.26, N 3.26; found: C 61.34, H 11.02, N 3.46.

Hexatriacontane-1,36-diyl-bis[2-(trimethylammonio)ethylphosphate] (**4d**). Yield: 0.54 g (62%). ^{1}H-NMR (400 MHz, CDCl$_3$/CD$_3$OD, 27 °C): δ = 0.98–1.09 (m, 64H, −O(CH$_2$)$_2$ (CH_2)$_{32}$(CH$_2$)$_2$O−), 1.31–1.38 (m, 4H, −OCH$_2$CH_2(CH$_2$)$_{32}$CH_2CH$_2$O−), 2.93 (s, 18H, 6× −CH_3), 3.29–3.32 (m, 4H, 2× NCH_2CH$_2$O−), 3.58 (q, J=6.6 Hz, 4H, −OCH_2(CH$_2$)$_{34}$CH_2O−), 3.91–3.97 (m, 4H, 2× NCH$_2$CH_2O−); MS (ESI): *m/z*: 869.7 [M$^+$+H], 891.6 [M$^+$+Na], 1761.1 [2M$^+$+Na]; elemental analysis calcd. (%) for C$_{46}$H$_{98}$N$_2$O$_8$P$_2$·2 H$_2$O: C 61.03, H 11.36, N 3.09; found: C 60.89, H 11.35, N 3.01.

Tetratriacontane-1,34-diyl-(12,12,13,13,14,14,15,15,16,16,17,17,18,18,19,19,20,20,21,21,22, 22,23,23-[D$_{24}$])-bis[2-(dimethylammonio)ethylphosphate] (**4e**). Yield: 0.31 g (75%); ^{1}H-NMR (500 MHz, CDCl$_3$/CD$_3$OD, 27 °C): δ = 1.13–1.24 (m, 36H, 2× −O(CH$_2$)$_2$(CH_2)$_9$−), 1.48–1.54 (m, 4H, 2× −OCH$_2$CH_2(CH$_2$)$_9$−), 2.76 (s, 12H, 4× −CH_3), 3.13–3.15 (m, 4H, 2× NCH_2CH$_2$O−), 3.76 (q, *J*=6.6 Hz, 4H, 2× −OCH_2(CH$_2$)$_{10}$−), 4.00–4.05 ppm (m, 4H, 2× NCH$_2$CH_2O−); ^{2}H-NMR (76.7 MHz, CHCl$_3$/CH$_3$OH, 27°C): δ = 1.29 ppm (s, −(CD_2)$_{12}$−); MS (ESI): *m/z*: 836.1 [M$^+$−H], 1672.0 [2M$^+$−2H], 838.9 [M$^+$+H], 860.7 [M$^+$+Na].

Tetratriacontane-1,34-diyl-(12,12,13,13,14,14,15,15,16,16,17,17,18,18,19,19,20,20,21,21,22, 22,23,23-[D$_{24}$])-bis[2-(trimethylammonio)ethylphosphate] (**4f**). Yield: 0.24 g (55%); ^{1}H-NMR (500 MHz, CDCl$_3$/CD$_3$OD, 27 °C): δ = 1.13–1.24 (m, 36H, 2× −O(CH$_2$)$_2$(CH_2)$_9$−), 1.47–1.52 (m, 4H, 2× −OCH$_2$CH_2(CH$_2$)$_9$−), 3.09 (s, 18H, 6× −CH_3), 3.45–3.47 (m, 4H, 2× NCH_2CH$_2$O−), 3.74 (q, *J*=6.6 Hz, 4H, 2× −OCH_2(CH$_2$)$_{10}$−), 4.08–4.12 ppm (m, 4H, 2× NCH$_2$CH_2O−); ^{2}H-NMR (76.7 MHz, CHCl$_3$/CH$_3$OH, 27°C): δ = 1.30 ppm (s, −(CD_2)$_{12}$−); MS (ESI): *m/z*: 865.9 [M$^+$+H], 887.7 [M$^+$+Na], 1753.4 [2M$^+$+2Na].

Methods

TEM

The cryo-transmission electron microscopy investigations were performed with a Zeiss 902A instrument, operating at 80 kV. Specimens were prepared by a blotting procedure, performed in a chamber with controlled temperature and humidity. A drop of the sample solution (1 mg ml^{-1}) was placed onto an EM grid coated with a perforated polymer film. Excess solution was then removed with a filter paper, leaving a thin film of the solution spanning the holes of the polymer film on the EM grid. Vitrification of the thin film was achieved by rapid plunging of the grid into liquid ethane held just above its freezing point. The vitrified specimen was kept below 108 K during both transfers to the microscope and investigation.

The negatively stained samples were prepared by spreading 5 µL of the dispersion onto a Cu grid coated with a formvar-film. After 1 min excess liquid was blotted off with filter paper and 5 µL of 1% aqueous uranyl acetate solution were placed onto the grid and drained off after 1 min. The dried specimens were examined with a Zeiss EM 900 transmission electron microscope.

X-ray diffraction

a) Powder pattern

A ground vacuum dried gel cake of dMe$_2$PE-C34-Me$_2$PE was filled into a glas capillary (∅ 1 mm) for investigations with a Guinier film camera (Huber) using quartz-monochromatized CuK$_\alpha$ radiation (4 h exposure time at room temperature, calibration of the film pattern with the powder pattern of Pb(NO$_3$)$_2$).

b) Partially aligned sample

A rectangular cuvette (0.8×0.4×1.8 cm^3) with 1 ml of a 2 mg ml^{-1} suspension of dMe$_2$PE-C34-Me$_2$PE was used to grow a gel cake of dMe$_2$PE-C34-Me$_2$PE with a shape of a rectangular parallelepiped being composed of stacked lamellae with relatively uniform orientation with respect to the stacking direction. The gel cake was placed on a microscopy cover glass. After a waiting time of three hours, the remaining trapped water within the gel cake was squeezed out.

2D patterns of the obtained partially aligned sample in two different orientations were recorded at room temperature with an area detector (HI-STAR, Siemens/Bruker) using Ni filtered CuK$_\alpha$ radiation.

^{2}H and ^{31}P solid-state NMR spectroscopy

The NMR experiments were performed on a BRUKER AVANCE-II spectrometer at a field of 9.4 T corresponding to Larmor frequencies of 161.98 and 61.43 MHz for ^{31}P and ^{2}H, respectively. For each spectrum 1000 signals were accumulated. The widths of the $\pi/2$ pulses were 2.0 µs (^{31}P) and 2.8 µs (^{2}H). For ^{2}H we used a solid-echo experiment which consists of two $\pi/2$ pulses with 2.8 µs duration; the delay between them was 20 µs. A compact gel cake of dMe_2PE-C34-Me_2PE containing approximately 20 w% of water was used either in contact with supernatant buffer solution or in the dried form. The concentration of the PC-C34-PC suspension was 10 mg ml^{-1} in water.

DSC

DSC measurements were performed using a MicroCal VP-DSC differential scanning calorimeter (MicroCal Inc. Northampton, MA). Before the measurements, the sample suspension (1 mg ml^{-1}) and the buffer reference were degassed under vacuum while stirring. A heating rate of 20 K h^{-1} was used, and the measurements were performed in the temperature interval from 2 to 95°C. To check the reproducibility, three consecutive scans were recorded for each sample. The buffer-buffer baseline was subtracted from the thermograms of the samples, and the DSC scans were evaluated using MicroCal Origin 7.0 software.

Small angle neutron scattering

SANS experiments were made using the SANS-1 instrument at the FGR1 research reactor at the GKSS Research Centre (Geesthacht, Germany). Details for the measurements were described recently.[S4, S5] The suspensions contained 1 mg ml^{-1} of the bolalipid in D_2O or D_2O buffer. The detailed data analysis is given below.

FT-IR

Infrared spectra were measured using a Bruker Vector 22 Fourier transform spectrometer with a DTGS-detector operating at 2 cm^{-1} resolution. The sample with a concentration of 50 mg·ml^{-1} was placed between two BaF_2 windows, which were separated by a 12 µm spacer for measurements in water or 300 mM acetate buffer. Before starting the temperature dependent measurements, each sample was equilibrated at 5°C for 2 h. IR-spectra were measured every 2 K in the temperature range from 5 to 95°C. After an equilibration time of 8 min 32 scans were recorded and accumulated. The corresponding spectra of the solvent were subtracted from the obtained sample spectra using the OPUS software supplied by Bruker.

X-ray diffraction

2D patterns of the partially aligned sample were recorded with an area detector (HI-STAR, Siemens/Bruker) using Ni filtered CuK_α radiation in two different orientations shown in Figure 1, orientation 1 with the incident X-ray beam perpendicular to the stacking direction of the lamellae (red arrow in Figure 1b), orientation 2 parallel to stacking direction (blue arrow in Figure 1b).
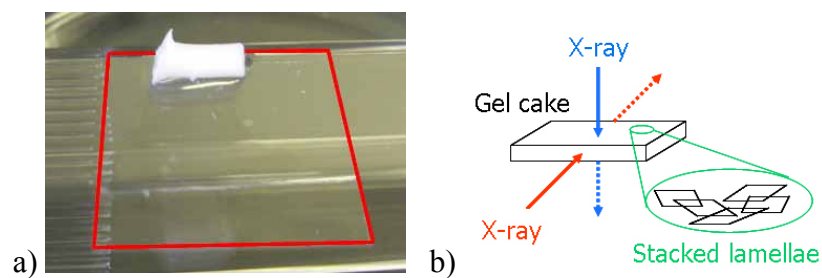
Fig. 1 a) Gel cake on a cover glass slide, b) orientation of the stacked lamellae in the gel cake and orientation of the X-ray beam in the two different diffraction experiments.
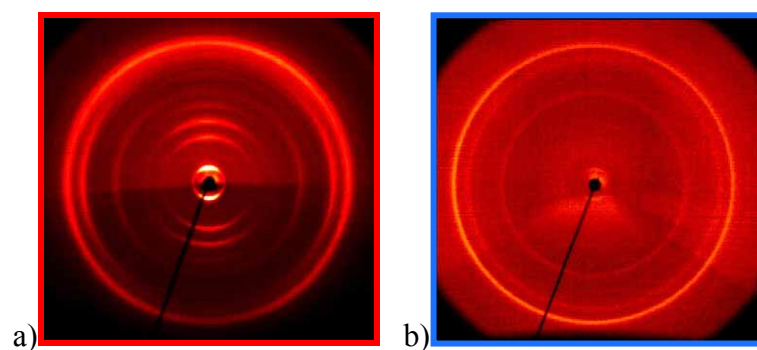
Fig. 2 2D XRD patterns of the gel cake in Figure 1, a) setting 1, b) setting 2.

a)

b)
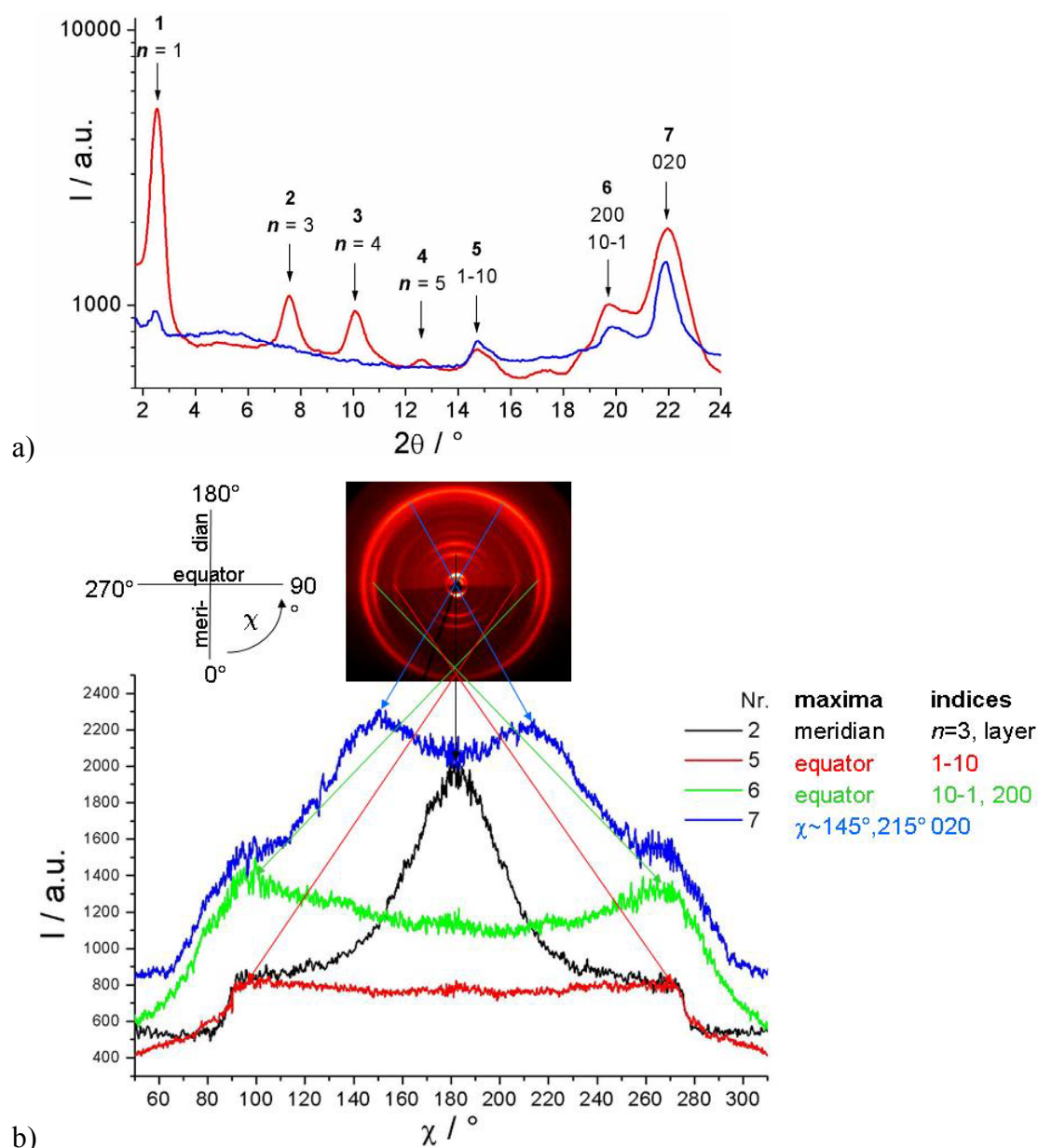
Fig. 3 a) Theta-scans for the patterns in Figure 2 showing the used reflection numbers as well as the order of the layer reflection in the small angle region and the indices according to the subcell of the hydrocarbon chains in the wide angle region (orientation 1: red line, orientation 2: blue line), b) Chi-scans for selected reflections (region below 90° and above 270° shadowed by the sample holder.

Table 1 Comparative compilation of crystallographic data derived from XRD measurements and molecular modeling (No. … reflection-no. used in the figures, I_{rel} … an estimate of the intensities from the X-ray patterns, n … order of the layer reflections, $2\theta_{obs}$ … observed diffraction angle (°), d_{obs} … observed d value (Å), d_{calc} … d value calculated from the subcell established by molecular modelling (Å), hkl … MILLER indices, I/I_{max} … relative intensity calculated from the subcell of hydrocarbon chains with $I_{max}(020) = 100$, subcell parameters: a = 8.9 Å, b = 8.12 Å, c = 5.17 Å, $\alpha = \beta = \gamma = 90°$).

No.	I_{rel}	n	$2\theta_{obs}$ 2D setting 1	d_{obs}/Å 2D setting 1	d_{obs}/Å 2D setting 2	d_{obs}/Å Guinier powder	hkl	d_{calc}/Å	I/I_{max}
1	vs	1	2.534	34.9	35.0	34.4			
2	m	3	7.577	11.7		11.5			
3	m	4	10.10	8.75		8.65			
4	w	5	12.59	7.03		6.89			
5	w		14.72	6.02	5.88	5.96	1-10	6.00	0.3
6	s		19.77	4.49	4.29	4.30	10-1	4.47	20.1
							200	4.45	20.6
7	vs		22.00	4.04	3.99	4.02	020	4.06	100
							11-1	3.91	13.2
							1-1-1	3.91	13.9
							210	3.90	13.3
							2-10	3.90	13.3

Molecular Modeling

Modeling and simulations of X-ray scattering patterns were performed using the *Materials Studio* software, release 4.1 (Accelrys Inc.).
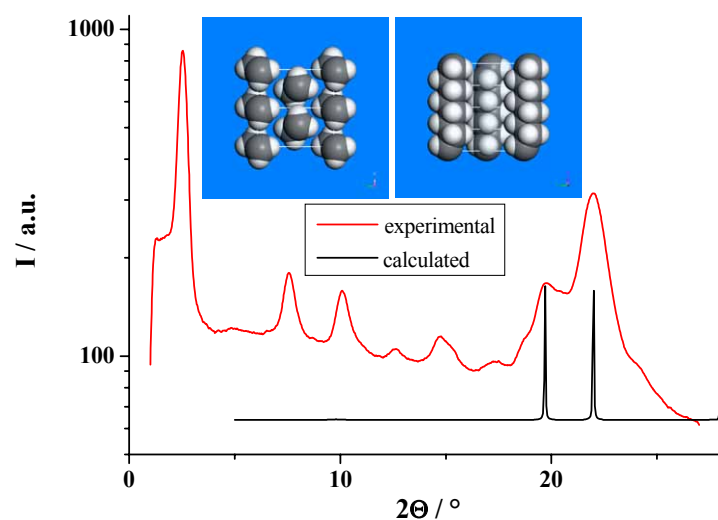

Fig. 4 Measured and calculated X-ray powder diffractograms of dMe$_2$PE-C34-Me$_2$PE with alkyl chains in a parallel arrangement. The inset shows eight subcells used for the calculation of the WAXD region. The subcell parameters are a = 4.52 Å, b = 9.01 Å, c = 2.583 Å, α = 90°, β = 90°, γ = 90°.

Table 2 Calculated **hkl**-reflections.

hkl	d_{calc}/Å	2Θ/ °	I/I_{max}
020	4.505	19.69	100
110	4.04	21.98	62.8
1-10	4.04	21.98	62.9

DSC measurements
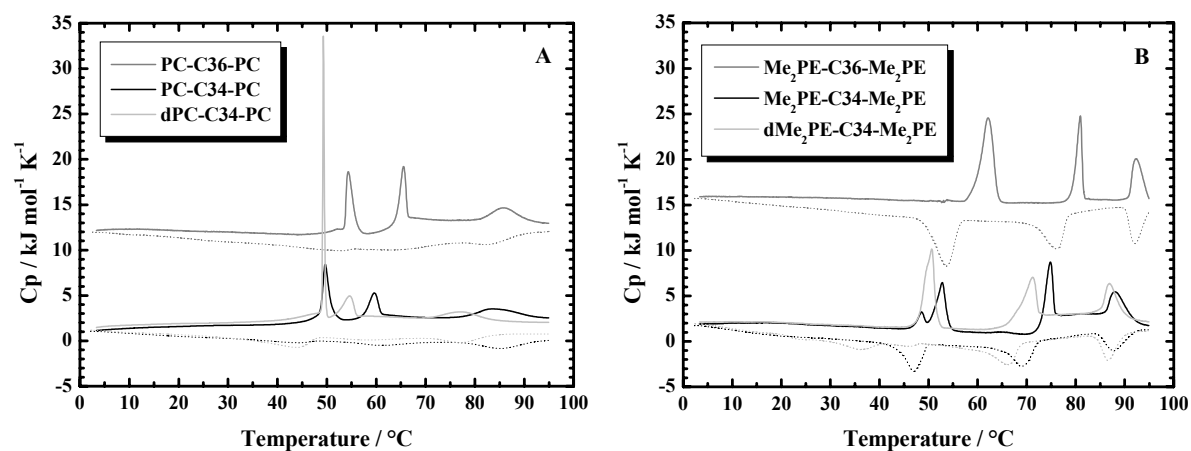
Fig. 5 DSC heating curves of (A) PC-C36-PC (1 mg ml^{-1}, shifted), PC-C34-PC (10 mg ml^{-1}) and dPC-C34-PC (10 mg ml^{-1}) and (B) Me$_2$PE-C36-Me$_2$PE (shifted), Me$_2$PE-C34-Me$_2$PE and dMe$_2$PE-C34-Me$_2$PE (1 mg ml^{-1}). Cooling curves are presented with dashed lines.

Cryo-TEM
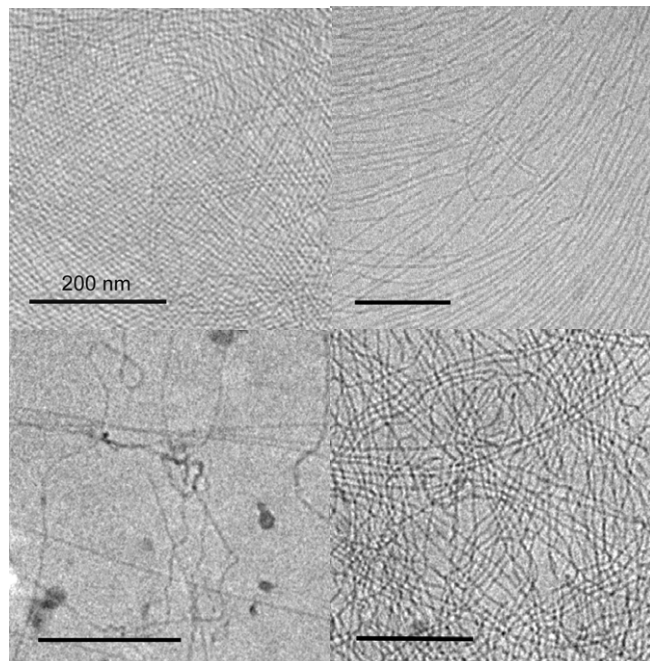
Fig. 6 Cryo-TEM image of aqueous suspensions (1 mg ml^{-1}) of PC-C36-PC (top left), PC-C34-PC (top right) and dMe$_2$PE-C34-Me$_2$PE (bottom right) quenched from 55°C. Me$_2$PE-C34-Me$_2$PE (bottom left) was quenched from 60°C. The bar corresponds to 200 nm.

SANS

Data analysis

It is possible to calculate the thickness of aggregates via GUINIER approximation [S6]. In the q range valid for a homogeneous membrane approximation, the scattering intensity can be given by:

$$(d\Sigma(q)/d\Omega)/c \sim q^{-2}\exp\left(-q^2 R_t^2\right),$$ (s1)

where R_t is gyration radius of thickness. In this approach, the R_t parameter is the absolute value of the slope of the KRATKY-POROD plot ($ln[I(q)q^2]$ vs q^2) and the thickness in homogeneous approximation, d_g, can be calculated as $d_g^2 = 12 R_t^2$.

Usually, only a limited interval of q can be used for the GUINIER approximation. Another possibility to get the thickness of aggregates via Indirect Fourier Transformation (IFT) was developed by GLATTER [S7]. The scattering intensities for flat aggregates are written in the form of the thickness pair distance distribution function $p_T(r)$:

$$(d\Sigma(q)/d\Omega)/c = (\frac{2\pi}{q^2})\pi\int_0^\infty p_T(r)\cos(qr)dr.$$ (s2)

The $p_T(r)$ function is given by [S6]:

$$p_T(r) = \frac{1}{2\pi M_S}\int \Delta\rho(r')\Delta\rho(r+r')dr',$$ (s3)

with r the coordinate in the *x*-direction, M_S corresponding to the mass per surface units of disc-like aggregates, and $\Delta\rho(r)$ is the scattering contrast (i.e., the difference between neutron scattering length densities of solute and solvent at point r). The distance distribution function $p_T(r)$ is estimated by applying the IFT method.

From $p_T(r)$ integral parameters of the thickness such as radius of gyration of thickness R_T and the mass per unit area M_S, can be calculated. The former is given by:

$$R_T = \left[\frac{\int_0^\infty r^2 p_T(r)dr}{\int_0^\infty p_T(r)dr}\right]^{1/2}.$$ (s4)

The thickness forward scattered intensity $I_T(0)$ is given by:

$$I_T(0) = 2\pi\int_0^\infty p_T(r)dr,$$ (s5)

from which M_S (in units g/cm^2) can be calculated via:

$$M_S = \frac{I_T(0)}{\Delta\rho^2} \; . \tag{s6}$$

In the case of rod like aggregates the scattering intensities can be expressed as:

$$\frac{d\Sigma(q)}{d\Omega} = \left(\frac{\pi}{q}\right) 2\pi \int_0^\infty \tilde{p}_{CS}(r) J_0(qr) r dr = \left(\frac{\pi}{q}\right) I_{CS}(q), \tag{s7}$$

where J_0 is the zeroth-order BESSEL function and $I_{CS}(q)$ the cross-sectional scattering intensity. The normalized cross-sectional distance distribution function $\tilde{p}_{CS}$ is given by:

$$\tilde{p}_{CS}(r) = \frac{c}{2\pi M_L} \int \Delta\rho(\mathbf{r})\Delta\rho(\mathbf{r}+\mathbf{r}')d\mathbf{r}', \tag{s8}$$

where the vectors $\mathbf{r}$ and $\mathbf{r}'$ are lying in the cross-section plane. $p_{CS}(r)$ can be deconvoluted further and a profile of scattering contrast can be obtained $\Delta\rho(r)$.

Similar to the way used for plane like aggregates, the radius of gyration of the cylindrical cross section ($R_{CS,g}$) and the mass per unit length M_L can be calculated from $p_{CS}(r)$. In the homogeneous approximation the mean radius of a cylindrical cross section is: $R_C = \sqrt{2} R_{CS,g}$.

Experimental data
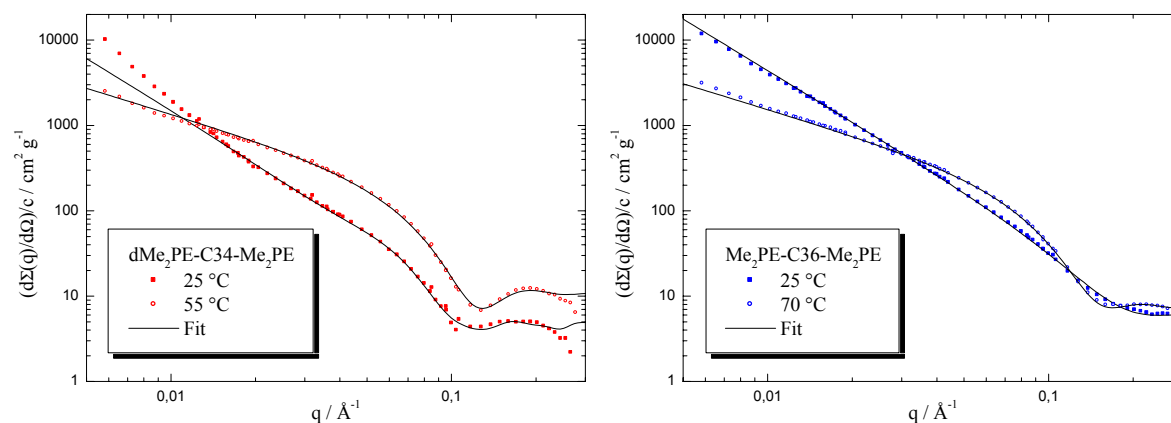
Fig. 7 Scattering intensities as a function of the scattering vector for dMe$_2$PE-C34-Me$_2$PE (left) and Me$_2$PE-C36-Me$_2$PE (right) (c = 1 mg ml^{-1}) at different temperatures (with model fits).

Table 3 Results of analysis for Me$_2$PE-C34-Me$_2$PE (c = 1 mg ml^{-1}) at 25 °C (below the first transition temperature).

| bolalipid	T [°C]	Slope analysis		GUINIER analysis			GLATTER analysis				
		Slope	Q [Å^{-1}]	R$_t$ [Å]	D [Å]	Q [Å^{-1}]	R$_t$ [Å]	D [Å]	I$_{(0)}$ [cm^{-1}]	D$_{max}$ [Å]	Q [Å^{-1}]
Me$_2$PE-C34-Me$_2$PE	25	2.49 ± 0.01	<0.05	15.4 ± 1.0	53	0.01-0.02	27.4 ± 0.7	96	8×10^{-5}	120	>0.01
dMe$_2$PE-C34-Me$_2$PE	25	2.46 ± 0.01	<0.05	15.6 ± 1.0	55	0.01-0.02	25.2 ± 0.8	87	7×10^{-5}	120	>0.01

Table 4 Results of analysis for Me$_2$PE-Cn-Me$_2$PE (c = 1 mg ml^{-1}) above the first transition temperature.

| bolalipid	T [°C]	GLATTER analysis			
		R$_C$ [Å]	I$_{(0)}$ [Å^{-1}cm^{-1}]	D$_{max}$ [Å]	Q [Å^{-1}]
Me$_2$PE-C34-Me$_2$PE	60	24.7	5.8×10^{-3}	55	whole
dMe$_2$PE-C34-Me$_2$PE	55	28.7	4.3×10^{-3}	55	whole

Table 5 Selected results of analysis for Me$_2$PE-C34-Me$_2$PE, dMe$_2$PE-C34-Me$_2$PE, and Me$_2$PE-C36-Me$_2$PE (c = 1 mg ml^{-1}) at different temperatures.

bolalipid	T [°C]	shape	R$_C$ [Å]	N$_{agg}$ [Å^{-1}], [nm^{-2}]	M$_L$ [g cm^{-1}], M$_S$ [g cm^{-2}]
Me$_2$PE-C34-Me$_2$PE	25	lamellae	/	1.74	2.36×10^{-7}
	60	fibers	24.7	1.34	1.82×10^{-13}
dMe$_2$PE-C34-Me$_2$PE	25	lamellae	/	0.97	1.35×10^{-7}
	55	fibers	28.7	/	/
Me$_2$PE-C36-Me$_2$PE	25	lamellae	/	1.44	2.02×10^{-7}
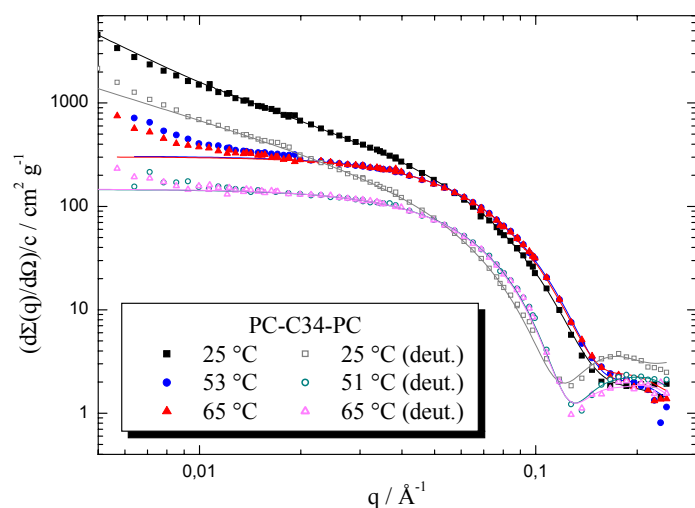
Fig. 8 Scattering intensities as a function of the scattering vector for PC-C34-PC and dPC-C34-PC ($c = 1$ mg ml^{-1}) at different temperatures (with model fits – solid lines).
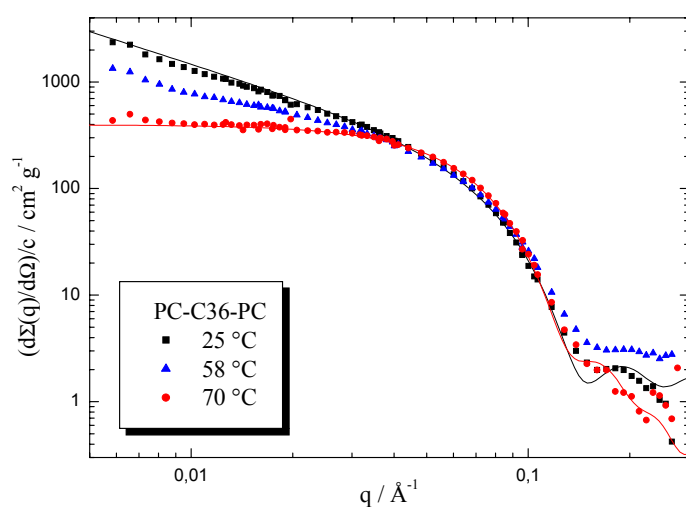

Fig. 9 Scattering intensities as a function of the scattering vector for PC-C36-PC ($c = 1$ mg ml^{-1}) at different temperatures (with model fits – solid lines).

Table 4 Selected results of analysis for PC-C34-PC, dPC-C34-PC and PC-C36-PC ($c = 1$ mg ml^{-1}) at different temperatures.

bolalipid	T [°C]	shape	radia [Å]	N_{agg} [Å^{-1}]	M, M_L [g], [g·cm^{-1}]
	25	rod-like fibers with flexibility	27.15	1.02	1.43×10^{-13}
PC-C34-PC	53	spheres with some fibers at low q	34.08	64.66	9.06×10^{-20}
	65	spheres with some fibers at low q	34.21	64.78	9.08×10^{-20}
	25	rod-like fibers	30.83	1.11	1.60×10^{-13}
dPC-C34-PC	51	spheres	36.28	66.69	9.62×10^{-20}
	65	spheres	36.54	67.19	9.69×10^{-20}
	25	stiff fibers, no flexibility is observed	26.30	1.01	1.46×10^{-13}
PC-C36-PC	58	some weak melting of fibers	Sample was not stable.		
	70	small micelles, most probably oblate shape	34.99	68.14	9.87×10^{-20}

FT-IR measurements
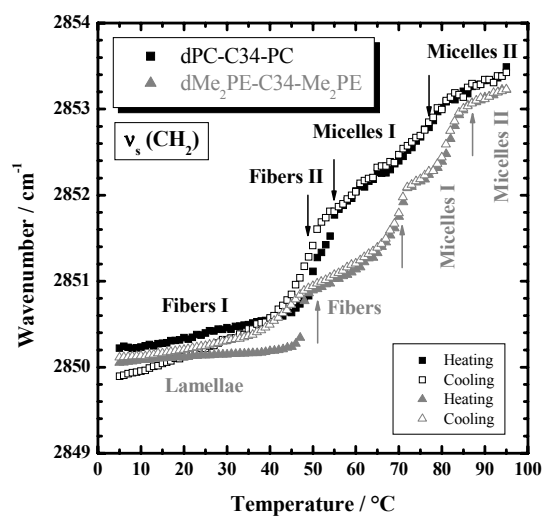
Fig. 10 Wavenumbers of the symmetric CH_2 stretching vibration as a function of temperature determined for suspensions of dPC-C34-PC and dMe$_2$PE-C34-Me$_2$PE. DSC transition temperatures are indicated by arrows.

References for Supporting Online Information

[S1] A. Meister, S. Drescher, I. Mey, M. Wahab, G. Graf, V.M. Garamus, G. Hause, H.-J. Mögel, A. Janshoff, B. Dobner, A. Blume, *J. Phys. Chem. B* **2008**, *112*, 4506.

[S2] K. Köhler, G. Förster, A. Hauser, B. Dobner, U.F. Heiser, F. Ziethe, W. Richter, F. Steiniger, M. Drechsler, H. Stettin, A. Blume, *Angew. Chem. Int. Ed*. **2004**, *43*, 245.

[S3] S. Drescher, A. Meister, A. Blume, G. Karlsson, M. Almgren, B. Dobner, *Chem. Eur. J.* **2007**, *13*, 5300.

[S4] A. Meister, M. Bastrop, S. Koschoreck, V. M. Garamus, T. Sinemus, G. Hempel, S. Drescher, B. Dobner, W. Richtering, K. Huber, A. Blume, *Langmuir*, **2007**, *23*, 7715-7723.

[S5] A. Meister, S. Drescher, V. M. Garamus, G. Karlsson, G. Graf, B. Dobner, A. Blume, *Langmuir*, **2008**, *24*, 6238-6246.

[S6] L. A. Feigin, D.I. Svergun, *Structure Analysis by Small-Angle X-Ray and Neutron Scattering*; Plenum Press: New York, 1987.

[S7] O. Glatter, *J. Appl. Cryst.* **1977**, *10*, 415.